

The Mechanism of Isoproterenol Hydrochloride-Induced Cardiac Arrhythmia and How Yangxin Dingji Capsule Alleviates These Effects by Modulating the CaMKII Pathway

Kexin Ma^{1,a}, Guoping Ma^{1,b}, Zan Xie^{2,c}, Mian Li^{1,d}, Ruijing Liang^{1,e},
Zijing Guo^{3,f}, Yameng Feng^{4,g}, Wenjie Liang^{4,h,*}, QiuHong Guo^{4,i,*}

¹Cardiovascular Department, The First Hospital of Hebei Medical University, Shijiazhuang, Hebei, China

²Hebei Yongfeng Pharmaceutical Co., Ltd, Shijiazhuang, Hebei, China

³Cardiovascular Department, Handan Central Hospital, Handan, Hebei, China

⁴Hebei University of Traditional Chinese Medicine, Shijiazhuang, Hebei, China

^a1715533072@qq.com, ^bmcp2006@163.com, ^cyxzyluck@163.com, ^d15227192961@163.com,

^e305914450@qq.com, ^f242305445@qq.com, ^gm863618642@163.com, ^hlwj712004@126.com,

ⁱqiuHong70105@163.com

*Corresponding author

Kexin Ma and Guoping Ma are contributed equally.

Abstract: Calcium/calmodulin-dependent protein kinase II (CaMKII) is critical for regulating cardiac electrophysiological functions. Research has shown that Yangxin Dingji capsule (YXDJ) significantly inhibits ventricular arrhythmia (VA). However, it is unclear whether YXDJ inhibits VA by regulating CaMKII. The aim of the present study was to elucidate the effects of YXDJ on the expression of CaMKII and sarco/endoplasmic reticulum Ca^{2+} ATPase 2 (SERCA2) and clarify the molecular mechanism by which YXDJ inhibits VA. Sixty healthy Sprague–Dawley rats were randomly divided into control, model, Propranolol, and YXDJ low-, medium- and high-dose groups and administered the corresponding treatment. The VA model was constructed by the isoproterenol hydrochloride (ISO) “6+1” method. Changes in the electrocardiograms of the rats were recorded, and pathomorphological changes were observed via hematoxylin–eosin staining. Enzyme-linked immunosorbent assays were used to measure cardiac troponin I, tumor necrosis factor- α , interleukin-1 β , interleukin-6, and myocardial Ca^{2+} levels and CaMKII activity. An automatic biochemical analyzer was used to measure the malondialdehyde, nitric oxide, and reduced glutathione levels and superoxide dismutase activity. Quantitative real-time polymerase chain reaction (PCR) was performed to detect SERCA2 and CaMKII gene expression, whereas the expression of CaMKII, phosphorylated phospholamban (P-PLB) and SERCA2 was evaluated via Western blotting. YXDJ was found to improve cardiac hypertrophy, reduce the incidence of VA, and protect cardiac tissue by alleviating inflammation and reducing oxidative stress levels in the body. The ISO-induced increases in CaMKII activity, CaMKII mRNA and protein expression, P-PLB protein expression and Ca^{2+} levels and decreases in SERCA2 mRNA and protein expression were effectively counteracted by YXDJ. YXDJ alleviated VA by reducing CaMKII expression and activating SERCA2, thereby reducing the Ca^{2+} load.

Keywords: calcium/calmodulin-dependent protein kinase II; sarco/endoplasmic reticulum Ca^{2+} ATPase 2; Yangxin Dingji capsule; ventricular arrhythmia; isoproterenol

1. Introduction

Ventricular arrhythmia (VA) is a common clinical condition that originates from the ventricle and does not include any myocardial tissue above the His bundle. VA is associated with high morbidity and mortality^[1] and includes ventricular premature beat (VP), ventricular tachycardia (VT) and ventricular fibrillation (VF). Epidemiological analysis has shown that 17 million people die of cardiovascular diseases worldwide each year, including 8.5 million who die from sudden cardiac death (SCD); additionally, 85% of SCD cases are caused by VA, particularly VT^[2,3]. Clinical VT treatments include drug therapy, and although drug therapy has shown considerable effects, it also has limitations, such as

cardiotoxicity and potentially arrhythmogenic effects, which greatly limit its clinical application. Therefore, new and effective drugs urgently need to be developed.

Isoproterenol hydrochloride (ISO) is a nonselective sympathomimetic catecholamine β -adrenergic receptor agonist that is often used to induce VA because it has positive inotropic, chronotropic, and dromotropic effects on myocardial tissue^[4]. As a key molecule downstream of ISO, calcium/calmodulin-dependent protein kinase II (CaMKII) is a multifunctional serine/threonine kinase that is widely involved in physiological processes, such as cardiac excitation–contraction coupling, excitation–transcription coupling and the mitochondrial function regulation, and is critical in regulating cardiac electrophysiological functions^[5,6].

The main active components of Yangxin Dingji capsule (YXDJ) include cinnamaldehyde, ginsenoside, Ophiopogon, and glycyrrhizic acid, which have beneficial effects on nourishing blood and restoring the pulse to prevent palpitation; thus, YXDJ has become a commonly used antiarrhythmic drug in clinical practice^[7,8]. Previous studies have shown that YXDJ significantly inhibits arrhythmias^[9,10]. Recent studies have shown the clear correlation between excessive CaMKII activation and the occurrence of VT^[6]. Additionally, oxidative stress induced by ISO can activate CaMKII via oxidation of methionines 281/282 (Met281/282), resulting in VA^[6,11]. However, whether YXDJ regulates CaMKII to inhibit VA and the mechanism by which YXDJ inhibits VT are unknown.

2. Materials and Methods

2.1 Animals

Specific pathogen-free (SPF) Sprague–Dawley rats weighing 100±150 g were purchased from Liaoning Changsheng Biotechnology Co., Ltd. (animal production license number: SCXK (Liao) 2020-0001; laboratory animal quality certificate: no. 210726200100262237). The experimental animals were kept in the Animal Laboratory of Hebei College of Traditional Medicine for one week at a temperature of 20±2°C with free access to food and water.

2.2 Drugs

YXDJ (06716120141) was purchased from Sinopharm Holding Group Hebei Yongfeng Pharmaceutical Co., Ltd. Propranolol hydrochloride (E181234) was obtained from Jiangsu Yabang Epsom Pharmaceutical Co., Ltd. Physiological saline (2007032007) was obtained from Shijiazhuang Siyao Co., Ltd. Sodium pentobarbital (Y0002194) was obtained from Sigma–Aldrich. ISO (I5627) and sodium pentobarbital (Y00021947) were procured from Sigma–Aldrich.

2.3 Reagents

Malondialdehyde (MDA; A003-1), superoxide dismutase (SOD; A001-3), nitric oxide (NO; A012-1) and glutathione (GSH; A006-2-1) detection kits were purchased from Nanjing Jiancheng Biological Co., Ltd. Ca^{2+} (C004-2-1), interleukin-6 (IL-6), interleukin-1 β (IL-1 β) and tumor necrosis factor alpha (TNF- α) detection kits were purchased from Beijing Xinbosheng Biotechnology Co., Ltd. The CaMKII kit (Cat# CY-1173) was obtained from CycLex (Japan). The phosphorylated phospholamban (P-PLB) primary antibody (P26678) was obtained from Cell Signaling Technology. Sarco/endoplasmic reticulum calcium-ATPase 2 (SERCA2; ab150435) and troponin (cTnI; ab256429) primary antibodies were obtained from Abcam. The CaMKII (ab52476) primary antibody was obtained from Abcam. Goat anti-rabbit IgG (IRDye® 800CW) secondary antibody was obtained from LI-COR (USA). RNA was extracted (G3013) by Servicebio.

2.4 Instruments

A physiological function experimental system (BL-420F) was purchased from Chengdu Taimeng Software Co., Ltd. Additionally, a refrigerated high-speed centrifuge (Fresco 21, Thermo Fisher Scientific, China), a fluorescence quantitative polymerase chain reaction (PCR) instrument (CFX, Bio-Rad), an UltraMicro spectrophotometer (NanoDrop 2000, Thermo Fisher Scientific), a high-speed refrigerated microcentrifuge (D3024R, DragonLab), a pathology graphic analysis system (DP72CCD, BX53 microscope, Olympus, Japan), and an infrared laser scanner (9141-00, Gene Company Ltd.) were used.

2.5 Dosing regimen

The content of YXDJ in each capsule was 0.5 g. The daily dosage of YXDJ for adult humans is 6–8 g. Thus, considering a conversion factor of 0.018, the daily dosage for rats would be 0.54–0.72 g/kg. In this study, low, medium and high doses (0.5 g/kg, 1.0 g/kg and 2.0 g/kg) of YXDJ were administered to the rats. Additionally, the daily dosage of propranolol hydrochloride for adult humans is 30–120 mg, which is equivalent to a dosage of 2.7–10.8 mg/kg for rats. In accordance with the literature, the dosage of propranolol hydrochloride used in this study was 15 mg/kg^[12,13].

2.6 Experimental grouping and model preparation

Sixty rats (weighing 100–150 g) were randomly divided into the control group and the following experimental groups: model, Propranolol, and YXDJ low-, medium- and high-dose groups, with 10 rats in each group. The low-, medium- and high-dose groups were given YXDJ at dosages of 0.5 g/(kg·d), 1.0 g/(kg·d) and 2.0 g/(kg·d), respectively. The rats in the Propranolol group were given propranolol hydrochloride at a dosage of 15 mg/(kg·d), and the control and model rats were given equal volumes of normal saline. The experimental period lasted 7 days, during which all the groups were administered the indicated treatments intragastrically. In addition, animal health and behavior were monitored daily and changes in body weight (BW) were measured every other day, and the dosage was adjusted as necessary.

In accordance with the study by Guo Z, a rat model of VA was constructed by injecting ISO in a "6+1" manner^[14]. Briefly, ISO was injected subcutaneously at a dosage of 5 mg/(kg·d) for 6 consecutive days, and on the 7th day, ISO (3 mg/kg) was injected intraperitoneally to induce VA. After accurately measuring the body BWs of the rats, the rats were anesthetized via the intraperitoneal injection of 2% sodium pentobarbital (40 mg/kg). Lead II ECG was subsequently performed, and the results were recorded for 1 h^[15]. Moreover, ISO was administered to induce VA, and ISO was administered 2 hours after intragastric administration^[16]. Finally, the dosage was adjusted according to the change in BW.

VT was defined as a sequence of a minimum of 4 consecutive VPs^[17]. Nonsustained ventricular tachycardia (NSVT) was defined as at least six but fewer than 15 nondriven consecutive VPs ($6 \leq \text{VP} < 15$). Ventricular tachycardia with 15 or more VPs ($\text{VP} \geq 15$) was defined as sustained ventricular tachycardia (SVT)^[18]. The arrhythmia score (severity) was assigned on the basis of the basic rating system, as follows: 0, no arrhythmia; 1, single VP; 2, two VPs; 3, three VPs or NSVT; 4, SVT; and 5, death^[14,18].

While still under anesthesia and after ECG monitoring was completed, Blood was collected from the SD rats via the femoral artery, the hearts were removed, and the rats were pronounced dead.

2.7 Calculation of the heart weight index (HWI)

Each heart was rinsed with 0.9% normal saline and weighed (HW). Then, the HWI was calculated as the ratio of HW to BW.

2.8 Measurement of serum cTnI levels

The blood was at room temperature for 2 hours and then centrifuged at 3000 rpm for 15 minutes at 4°C to obtain the supernatant (serum), which was frozen at -80°C. Serum samples were analyzed in strict accordance with the instructions of the cTnI detection kit provided by Abcam. The absorbance of each serum sample was measured, and these values were converted to expression levels.

2.9 Detection of oxidative stress and inflammatory factors in the serum

The contents of SOD, MDA, NO and GSH in the separated serum were detected with an automatic biochemical analyzer, and the absorbance of each serum microplate measured, and these values were converted to expression levels. Serum samples were subjected to enzyme-linked immunosorbent assays (ELISAs) using the double antibody sandwich method according to the instructions of the IL-6, IL-1 β and TNF- α detection kits provided by Beijing Xinbosheng Technology Co., Ltd. The absorbance of each serum sample was measured, and these values were converted to expression levels.

2.10 Pathological changes in myocardial tissue observed via hematoxylin–eosin (HE) staining

The obtained myocardial tissue sections were immediately cleaned with normal saline, fixed in 10% neutral buffered formalin, embedded in paraffin, dehydrated with alcohol, sliced, and stained with HE. The pathological changes and inflammatory cell infiltration in the myocardial tissue were observed under a high-power microscope.

2.11 Measurement of Ca^{2+} levels in myocardial tissue

First, 100 mg of ventricular tissue was accurately weighed, physiological saline was added at a weight (g): volume (ml) ratio of 1:4, and the sample was mechanically homogenized in an ice–water bath. The sample was subsequently centrifuged for 15 minutes at 12000 rpm, after which the 25% of the supernatant was stored at -80°C . The Ca^{2+} content in the tissue supernatant was determined by measuring the absorbance of each tissue supernatant sample in a microplate.

2.12 Measurement of CaMKII activity in cardiomyocytes

An ELISA was used to examine the tissue supernatant samples according to the instructions of the CaMKII detection kit (CycLex, Japan). The absorbance of each tissue supernatant sample was measured and converted to CaMKII activity.

2.13 Detection of CaMKII, P-PLB, and SERCA2 protein expression in cardiomyocytes by Western blotting

Rat left ventricle tissue was added to an equal amount of a mixture containing protease inhibitors, phosphatase inhibitors and RIPA lysis solution (strong) for 30 min of incubation before centrifugation at 12,000 rpm for 20 min at 4°C . The supernatant was collected, and the proteins in the supernatant were quantified with a BCA kit. Next, the proteins were subjected to a 5% concentrated gel and 10% and 12% separation gels before being transferred to PVDF membranes for 25–35 min at a constant voltage of 25 V. Then, 5% and 15% skim milk, prepared in TBST, were added to the membrane for incubation at room temperature for 60 min. Subsequently, CaMKII, P-PLB (1:1000), SERCA2 (1:5000) and GAPDH (1:3000) primary antibodies were added, and the membranes were incubated overnight at 4°C . The next day, the membrane was washed 3 times with TBST for 8 min each time, incubated with IRDye-labeled secondary antibodies (1:10000) for 60 min at room temperature, and washed 3 times with TBST for 8 min each time. Then, ImageJ software was used to analyze and measure the gray values of the bands using GAPDH as the internal reference.

2.14 Detection of CaMKII δ and SERCA2 expression in myocardial tissue via real-time PCR

The extracted RNA was reverse transcribed into cDNA and amplified. Each PCR (20 μL) was performed under the following conditions: predenaturation at 95°C for 2 min; two-step annealing (95°C for 10 s, 60°C for 1 min) for 44 cycles; and extension at 95°C for 15 s, 60°C for 60 s, and 95°C for 15 s. After amplification, the Cq values were obtained for the target gene and internal reference gene GAPDH, and ΔCq was calculated by subtracting the Cq value of the internal reference gene (GAPDH) from the Cq value of the target gene. Then, the formula $Q=2^{-\Delta\text{Cq}}$ was used to calculate the Q value of each target gene, and subsequently, the mean Q value. Finally, for each target gene, the ratio of Q value/mean Q value was calculated to give the relative quantitative value (RQ value) of the target gene, which was used for statistical analysis.

Gene	Sequence (5'–3')	
GAPDH	Forward	CTGGAGAAACCTGCCAAGTATG
	Reverse	GGTGAAGAATGGGAGTTGCT
SERCA2	Forward	AAGCATACTGACCCTGTCCCTG
	Reverse	CCACCACCACTCCCATAGCTT
CaMKII δ	Forward	CAAACTACTGTAATCCACAACCCTG
	Reverse	CGTGTAAGCCTCGAAGTCCC

2.15 Statistical analysis

Parametric statistical tests were used for data analysis, and the results are presented as the means \pm SDs. SPSS 21.0 statistical software was used for data analysis. One-way analysis of variance was used to compare the differences among groups. Tukey's test was used for comparisons between two groups, while the Kruskal–Wallis H rank test was used for statistical analysis of the arrhythmia score (severity). $P < 0.05$ was considered to indicate a significant difference.

3. Results

3.1 General condition of the rat

Compared with those in the control group, the rats in the model group exhibited decreased food and water intake, a slower rate of weight increase, and a weakened response. Compared with those in the model group, the rats in the Propranolol group displayed increased food and water intake and quality and enhanced responses. None of the rats in the control group or Propranolol group died, whereas three rats in the model group died. None of the rats in any of the groups died within the first 6 days. However, on the 7th day, when lead II ECG was performed, three rats died in the model group, two died in each the YXDJ low- and medium-dose groups, and one died in the YXDJ high-dose group. All of these rats died of VF.

3.2 HWIs in each group

Compared with that in the control group, the HWI in the model group was significantly greater ($P < 0.01$). Additionally, compared with that in the model group, the HWIs in the experimental groups were significantly lower ($P < 0.01$ or $P < 0.05$) (see Table 1).

Table 1: Effects of YXDJ on the HWIs of rats in different groups (means \pm SDs)

Group	BW	HW	HWI
Control	221.90 \pm 15.67	0.774 \pm 0.069	0.349 \pm 0.020
Model	222.86 \pm 14.84	1.130 \pm 0.104**	0.506 \pm 0.015**
Propranolol	229.30 \pm 12.04	0.973 \pm 0.044 ^{##}	0.425 \pm 0.014 ^{##}
YXDJ low	233.00 \pm 9.20	1.109 \pm 0.042	0.475 \pm 0.013 [#]
YXDJ medium	235.38 \pm 11.96	1.065 \pm 0.064	0.454 \pm 0.023 ^{##}
YXDJ high	229.89 \pm 10.30	0.993 \pm 0.067 ^{##}	0.432 \pm 0.016 ^{##}

The data are presented as the means \pm standard errors of the means. ** $P < 0.01$ comparing the control group with the model group; # $P < 0.05$, ## $P < 0.01$ comparing the experimental groups with the model group.

3.3 Arrhythmia scores (severity) in each group

The arrhythmia score (severity) in the model group was significantly greater than that in the control group ($P < 0.01$). Compared with that in the model group, the arrhythmia score (severity) in the Propranolol group was significantly lower ($P < 0.05$) but the arrhythmia scores (severity) in the YXDJ low-, medium- and high-dose groups were not significantly lower ($P > 0.05$) (see Table 2).

Table 2: Comparison of the arrhythmia scores (severity) of each group

Group	none	VPB	double VPBs	three VPBs or NSVT	SVT	death	Total score
Control	8	2					2
Model				1	6	3	42**
Propranolol	2	1	1	2	4		25 [#]
YXDJ low				2	6	2	40
YXDJ medium	1	1	2		4	2	29
YXDJ high	1	2	1	1	4	1	28

Notes: 0, no arrhythmia; 1, single VP; 2, two VPs; 3, three VPs or NSVT; 4, SVT; and 5, death.
 **P<0.01 control group vs. the model group; [#]P<0.05 experimental groups vs. the model group.

3.4 Incidence of VA in each group

Compared with those in the control group, the VT and VP incidence rates in the model group were significantly greater ($P<0.01$). However, compared with those in the model group, the VT and VP incidence rates in the Propranolol and YXDJ high-dose groups were significantly lower ($P<0.05$), but the VT and VP incidence rates in the YXDJ low- and medium-dose groups were not significantly lower ($P>0.05$) (see Figure 1).



Figure 1: Incidence of VA in each group. The control rats had normal electrocardiograms. The electrocardiograms of the rats in the model group revealed mainly VT. of the electrocardiograms of the rats in the Western medicine and experimental groups revealed significant improvements in VT severity, and some of the rats showed normal performance. The incidence rates of VT in the control, model, Propranolol, and YXDJ low-, medium- and high-dose groups were 0%, 100%, 40%, 87.5%, 50% and 44.4%, respectively; and the incidence rates of VP in the control, model, Propranolol, YXDJ low-, medium- and high-dose groups were 0%, 100%, 50%, 87.5%, 75% and 66.7%, respectively.

3.5 Myocardial injury in each group

Compared with that in the control group, the cTnI level in the model group was significantly greater ($P<0.01$), whereas compared with that in the model group, the cTnI levels in the Propranolol and

YXDJ medium- and high-dose groups were significantly lower ($P<0.01$ or $P<0.05$) (see Figure 2).

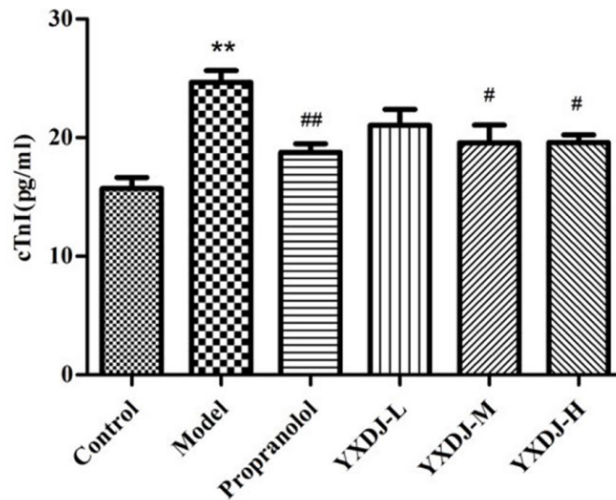


Figure 2: Myocardial injury in each group. ** $P<0.01$ control group vs. the model group; # $P<0.05$ and ## $P<0.01$ experimental groups vs. the model group.

3.6 Oxidative stress levels in each group

Compared with those in the control group, in the model group, the SOD and GSH levels were significantly lower ($P<0.01$), and the MDA and NO levels were significantly greater ($P<0.01$). Furthermore, compared with those in the model group, Propranolol and YXDJ high-dose groups, the levels of SOD and GSH were significantly greater ($P<0.01$), and the levels of MDA and NO significantly lower ($P<0.05$ or $P<0.01$). The levels of these four indexes also changed in the YXDJ medium- and low-dose groups (see Figure 3).

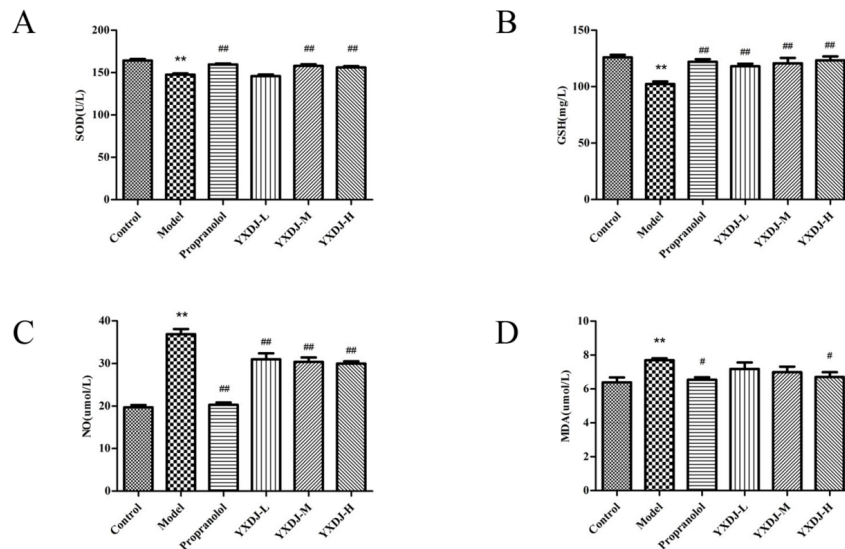


Figure 3: Levels of oxidative stress indicators in rat serum. ** $P<0.01$ control group vs. the model group; # $P<0.05$ and ## $P<0.01$ experimental groups vs. the model group.

3.7 Expression of inflammatory factors in each group

Compared with those in the control group, the levels of TNF- α , IL-6 and IL-1 β in the model group were significantly greater ($P<0.01$). Additionally, compared with those in the model group, the levels of these three indexes in the Propranolol group were significantly lower ($P<0.01$ or $P<0.05$), whereas the levels of IL-6 and IL-1 β in the YXDJ medium- and high-dose groups were significantly lower ($P<0.01$ or $P<0.05$) (see Figure 4).

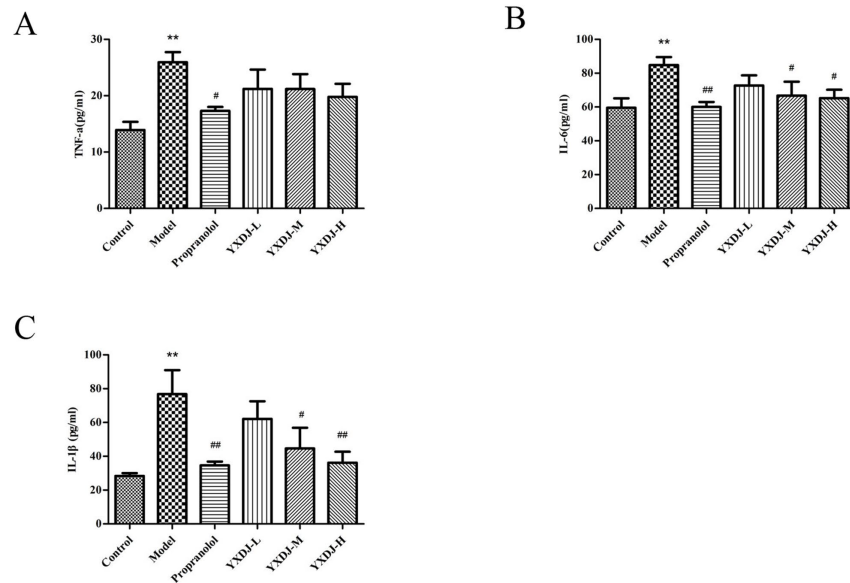


Figure 4: Expression of inflammatory factors in rat serum. ** $P < 0.01$ control group vs. the model group; # $P < 0.05$ and ## $P < 0.01$ experimental groups vs. the model group.

3.8 Morphology of the myocardial tissue in each group

HE staining revealed no obvious abnormalities in the myocardial tissue of the rats in the control group. Moreover, compared with those in the control group, the myocardial tissues of the rats in the model group presented edema, necrosis, lysis and inflammatory cell infiltration. The myocardial tissues of the rats in the Western medicine group displayed significant improvements. Notably, the YXDJ groups also presented different degrees of improvement that were dose dependent, with the effects in the YXDJ high-dose group being the most obvious (see Figure 5).

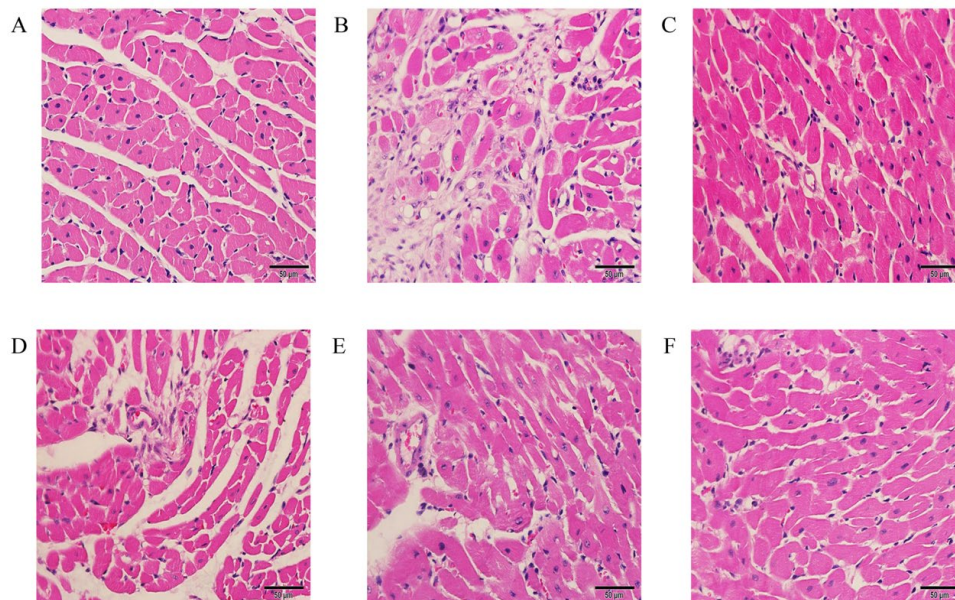


Figure 5: Morphology of the myocardial tissue in each group. A: Control group; B: model group; C: Propranolol group; and D, E, F: YXDJ low-, medium-, and high- groups.

3.9 CaMKII activity in each group

Compared with that in the control group, the CaMKII activity in the model group was significantly increased ($P < 0.01$). Additionally, compared with that in the model group, the CaMKII activity in the Propranolol, YXDJ medium- and high-dose groups was significantly lower ($P < 0.05$) (see Figure 6).

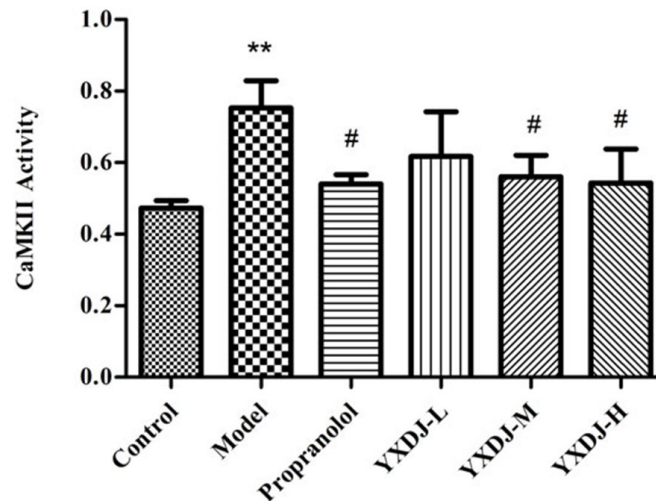


Figure 6: CaMKII activity in rat cardiomyocytes. ** $P < 0.01$ control group vs. the model group; # $P < 0.05$ experimental groups vs. the model group.

3.10 CaMKII δ mRNA expression in each group

Compared with that in the control group, the mRNA expression of CaMKII δ in the model group was significantly greater ($P < 0.01$). Furthermore, compared with that in the model group, CaMKII δ mRNA expression in the Propranolol group ($P < 0.01$) and YXDJ groups was lower ($P < 0.01$ or $P < 0.05$) (see Figure 7).

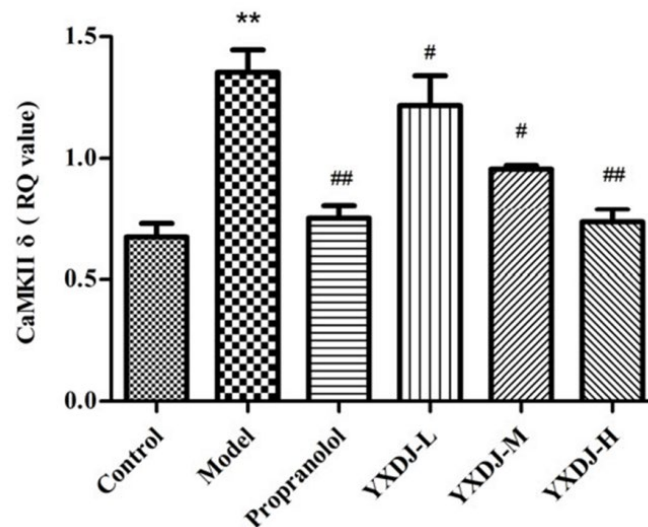


Figure 7: Expression of CaMKII δ mRNA in rat myocardial tissue measured via real-time PCR. ** $P < 0.01$ control group vs. the model group; # $P < 0.05$, ## $P < 0.01$ experimental groups vs. the model group.

3.11 CaMKII protein expression in each group

Compared with that in the control group, CaMKII expression in the model group was significantly greater ($P < 0.01$). Additionally, compared with that in the model group, the CaMKII expression levels in the Propranolol and YXDJ low-, medium- and high-dose groups were significantly lower ($P < 0.01$ or $P < 0.05$) (see Figure 8).

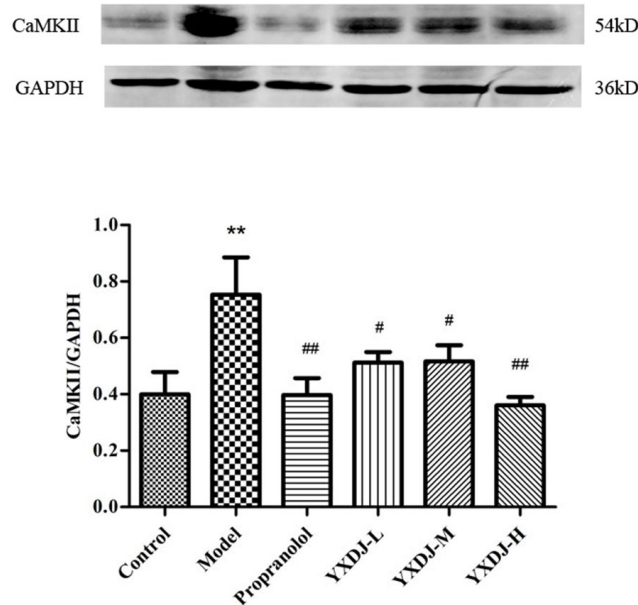


Figure 8: Western blot analysis of CaMKII expression in rat cardiomyocytes. ** $P < 0.01$ control group vs. the model group; # $P < 0.05$, ## $P < 0.01$ experimental groups vs. the model group.

3.12 SERCA2 mRNA expression in each group

Compared with that in the control group, the SERCA2 mRNA expression level in the model group was significantly lower ($P < 0.01$). Moreover, compared with that in the model group, the SERCA2 mRNA expression levels in the Propranolol and YXDJ low-, medium- and high-dose groups were significantly greater ($P < 0.01$ or $P < 0.05$) (see Figure 9).

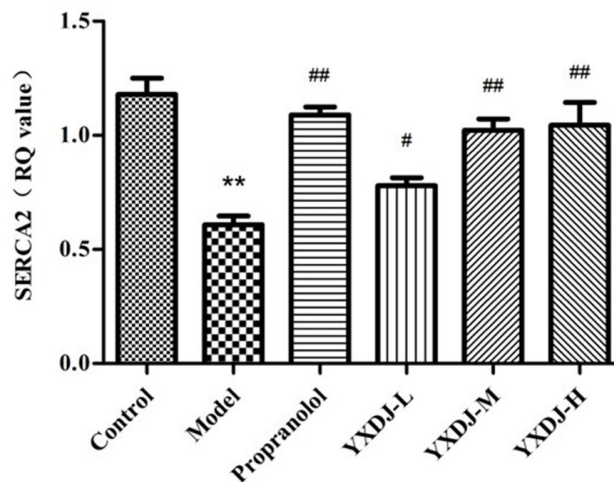


Figure 9: Real-time PCR analysis of SERCA2 mRNA expression in rat myocardial tissue. ** $P < 0.01$ control group vs. the model group; # $P < 0.05$, ## $P < 0.01$ experimental groups vs. the model group.

3.13 SERCA2 protein expression in each group

SERCA2 protein expression was significantly lower in the model group than in the control group ($P < 0.01$). Additionally, compared with that in the model group, SERCA2 protein expression in the Propranolol and YXDJ medium- and high-dose groups was significantly greater ($P < 0.01$ or $P < 0.05$) (see Figure 10).

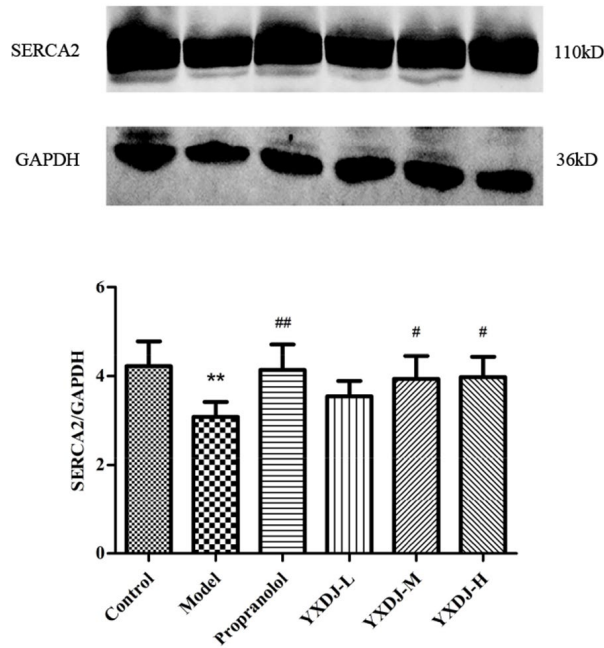


Figure 10: Western blot analysis of SERCA2 expression in rat cardiomyocytes. ** $P < 0.01$ control group vs. the model group; # $P < 0.05$, ## $P < 0.01$ experimental groups vs. the model group.

3.14 P-PLB protein expression in each group

Compared with that in the control group, the P-PLB protein expression level in the model group was significantly greater ($P < 0.01$). Compared with that in the model group, the P-PLB protein expression levels in the Propranolol and YXDJ low-, medium- and high-dose groups were significantly lower ($P < 0.01$ or $P < 0.05$) (see Figure 11).

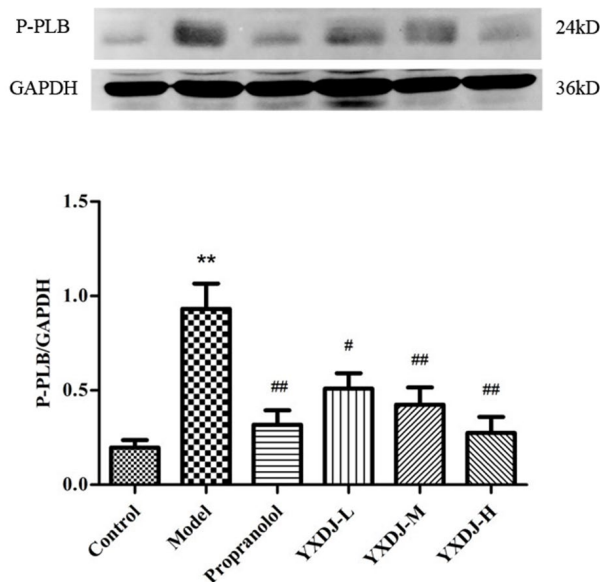


Figure 11: Western blot analysis of P-PLB expression in rat cardiomyocytes. ** $P < 0.01$ control group vs. the model group; # $P < 0.05$, ## $P < 0.01$ experimental groups vs. the model group.

3.15 Ca^{2+} levels in each group

Compared with that in the control group, the Ca^{2+} level in the myocardial tissue in the model group was significantly greater ($P < 0.01$). Furthermore, compared with that in the model group, the Ca^{2+} levels

in the myocardial tissue in the Propranolol and YXDJ medium- and high-dose groups were significantly lower ($P<0.01$) (see Figure 12).

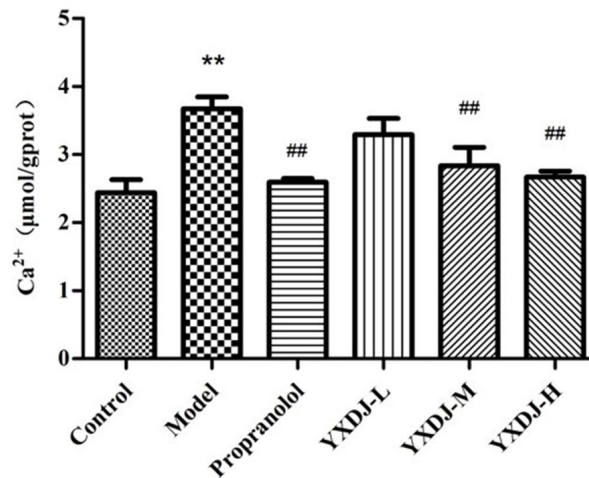


Figure 12: Comparison of Ca^{2+} levels in rat myocardial tissue. ** $P<0.01$ control group vs. the model group; ## $P<0.01$ experimental groups vs. the model group.

4. Discussion

Recent research on the pathogenesis of VA. VA is a highly lethal arrhythmia that involves multiple ion channels. More than 10% of patients with acute myocardial infarction develop VA, and particularly VT and VF, before being admitted to the hospital and have very low survival rates^[2]. Recent studies on the mechanism of VA have focused mainly on reentry and triggering events, which are caused mainly by early afterdepolarizations (EADs) and delayed afterdepolarizations (DADs). Ca^{2+} plays an important role in excitation–contraction coupling in cardiomyocytes. When Ca^{2+} enters the cytoplasm via the sarcoplasmic reticulum (SR), the myocardium becomes contractile. During diastole, cytoplasmic Ca^{2+} is pumped back to the SR by SERCA2 or excreted from cells by the Na^{+} - Ca^{2+} exchanger (NCX). An inward current (INCX) can be generated when Ca^{2+} is excreted from cells through NCX^[19]. When the INCX is high enough to depolarize the cardiac membrane, voltage-dependent sodium ion channels are activated, and DADs are induced^[20]. When the L-type Ca^{2+} channel (LTCC)-mediated L-type calcium current or INCX is greater than the outgoing K^{+} current, the action potential duration is prolonged, which can lead to EAD. When the abnormal depolarization reaches the membrane potential threshold, a spontaneous action potential can be generated between two conventional action potentials, constituting the occurrence of VA^[19,20]. Our previous research revealed that a VA model can be constructed by injecting ISO using the "6+1" method^[14].

Relationship between the β -adrenergic receptor and CaMKII activation. β -Adrenergic receptor stimulation can stimulate myocardial tissue to produce many reactive oxygen species (ROS), such as superoxide, hydrogen peroxide and hydroxyl free radicals^[21]. High levels of ROS disrupt the physiological balance of the antioxidant defense system, leading to oxidative stress^[21]. CaMKII can be oxidized at Met281/282 to produce OX-CaMKII, whose expression level reflects the activity of CaMKII^[5,22]. An increasing number of studies have shown that β -adrenergic receptor stimulation leads to the cAMP/PKA-mediated autophosphorylation of CaMKII at Thr287 and that NO, a signaling molecule generated during β -adrenergic receptor stimulation, can trigger S-nitrosylation of CaMKII^[23,24]. Moreover, β -adrenergic receptor activation can induce Ca^{2+} release mediated by PLC-IP₃, after which Ca^{2+} combines with CaM (a ubiquitous intracellular Ca^{2+} binding protein) to form the Ca^{2+} /CaM complex, which directly leads to CaMKII activation^[6]. Propranolol, a β -adrenergic blocker, can block the above effects. Studies conducted by Yang M et al. and Macala K et al. showed that 15 mg/kg propranolol can stabilize membranes and plays an important role in Ca^{2+} homeostasis^[12,13]. These effects of propranolol are beneficial for protecting myocardial cells and antagonizing arrhythmias (see Figure 13).

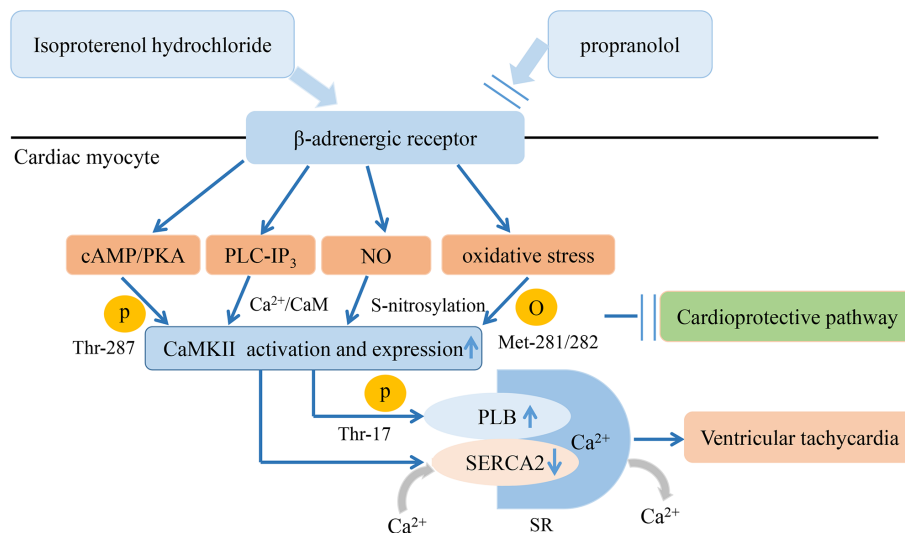


Figure 13: Illustration of the proposed role of β -AR signaling during VA in cardiac muscle. This scheme shows the proposed role of β -AR signaling in the hearts of ISO-treated mice. β -AR signaling is activated by ISO, leading to the CaMKII-mediated phosphorylation of PLN (Thr17) and a reduction in SERCA2 levels (left). Propranolol (right) protects the heart from VA.

YXDJ improves ISO-induced VA. YXDJ is an improved preparation based on Zhigancao decoction, which is composed of licorice, *Rehmannia glutinosa*, ophiopogonin, red ginseng, donkey-hide gelatin, black sesame, jujube, cinnamon stick and ginger. This formula has notable antiarrhythmic effects, as it can regulate the cardiomyocyte electrophysiological conduction and the excitability of ectopic pacemakers while reducing the heart rate and myocardial oxygen consumption^[9,10]. Furthermore, ophiopogonin can alleviate oxidative stress and the inflammatory response and maintain Ca^{2+} homeostasis^[7,25]. The main active components of cinnamon sticks and licorice are cinnamic acid and glycyrrhizic acid, respectively, both of which have anti-inflammatory and antioxidant effects and can effectively inhibit LTCCs^[8]. Ginsenoside, the main active substance in red ginseng, has electrophysiological effects on the heart that are similar to those of amiodarone, which can regulate ion channels^[26,27]. On the basis of the incidences of VP and VT observed in this study, high-dose YXDJ significantly reduced the frequency of VA and the severity of arrhythmia.

YXDJ reduces ISO-induced myocardial hypertrophy and myocardial injury. ISO can regulate myocardial blood volume by interacting with β receptors on cardiomyocytes. Therefore, ISO is widely used to stimulate myocardial hypertrophy^[28,29]. Panda S et al. reported that ISO can increase the HWI^[30]. In this study, the HWI was significantly reduced in the YXDJ groups, indicating that YXDJ improved ISO-induced myocardial hypertrophy in rats. Moreover, oxidative stress induced by ISO can cause irreversible damage to the myocardial cell membrane and mitochondrial dysfunction, leading to myocardial injury^[21,31]. Moreover, myocardial injury can modulate the sympathetic nervous system, promote the release of catecholamines, and lead to myocardial scarring and fibrosis, which further changes the generation and conduction of electrical signals in the myocardium and increases susceptibility to VA^[32-34]. cTnI is a heart-specific protein that is transiently elevated after ISO-induced acute myocardial injury; thus, its expression reflects the degree of myocardial damage^[35]. This study revealed that ISO intervention increases cTnI expression, which was also shown by Thangaiyan R et al.^[36]. Notably, the medium and high doses of YXDJ significantly decreased cTnI expression, indicating that YXDJ can effectively reduce the degree of myocardial cell injury. HE staining revealed significant inflammatory cell infiltration, edema, deformation, and necrosis in the myocardial tissue of ISO-induced SD rats, similar to the findings of Ping^[37]. In the YXDJ groups, these pathological changes were significantly improved, indicating that YXDJ protects cardiomyocytes.

YXDJ reduces the degree of oxidative stress in myocardial tissue. As the primary targets of oxidative stress, phospholipids and fatty acids on the cell membrane are converted into lipid peroxides under the action of ROS^[38,39]. As one of the end products of lipid peroxidation, MDA is usually considered a marker of oxidative stress, and its expression is positively correlated with the degree of oxidative stress^[21,38,39]. SOD is an endogenous antioxidant enzyme that converts superoxide into hydrogen peroxide, while GSH can react with different free radicals and disulfides, thereby protecting the body from damage caused by ROS^[31]. Previous studies have shown that ISO intervention increases

MDA levels and reduces SOD and GSH levels^[38,40]. Furthermore, myocardial injury can promote the production of inducible nitric oxide synthase (iNOS), an enzyme important for NO production. Large amounts of NO can react with superoxide radicals to produce the more potent oxidant peroxynitrite. Thus, ISO enhances oxidative stress^[41,42]. Previous studies have shown that ISO administration can increase serum MDA and NO levels and reduce SOD and GSH levels^[38]. In this study, the levels of MDA and NO in the serum decreased in the YXDJ groups, while the SOD and GSH levels increased, suggesting that YXDJ may protect myocardial tissue through antioxidant mechanisms.

YXDJ alleviates myocardial tissue inflammation. Myocardial injury promotes macrophage activation, which triggers the inflammatory response and the release of proinflammatory cytokines, such as TNF- α , IL-1 β and IL-6. Collectively, oxidative stress and proinflammatory cytokines exacerbates myocardial injury^[21,39,41]. TNF- α is synthesized in large quantities in the early stage of myocardial injury, and its main functions include immune cell regulation, cardiac function inhibition and the induction of IL-1 β release^[43,44]. IL-1 β can increase endothelial cell permeability and stimulate the release of chemokines, leading to the accumulation of neutrophils and macrophages in damaged myocardial tissue and further triggering an inflammatory response^[45]. IL-6 is a pleiotropic cytokine involved in pathological processes such as cardiac inflammation and dysfunction. In the present study, serum levels of proinflammatory cytokines were significantly increased after ISO intervention, which is consistent with the findings of Sherein F El-Sayed et al.^[46]. In our study, the release of proinflammatory cytokines in the rat myocardium was significantly reduced in the YXDJ groups, indicating that YXDJ protects the myocardium by mitigating the inflammatory response.

YXDJ may regulate CaMKII activity and expression by relieving oxidative stress and the inflammatory response. There are four subtypes of CaMKII, α , β , γ and δ , among which CaMKII δ is expressed mainly in cardiomyocytes^[11]. Once activated, CaMKII regulates LTCCs, sarcoplasmic Ca²⁺ release channels, SERCA2, and PLB and participates in the regulation of cardiomyocyte electrophysiology^[22,47]. Previous studies have shown that oxidative stress induced by ISO increases CaMKII δ mRNA expression, CaMKII expression and CaMKII activity^[48]. Our study revealed that YXDJ significantly reduced CaMKII δ mRNA expression, CaMKII expression and CaMKII activity by modulating the antagonism of calcium ion regulatory proteins, thereby alleviating oxidative stress and the inflammatory response and inhibiting VA.

The mechanism by which YXDJ antagonizes VA may be related to its upregulation of SERCA2 and ability to decrease the cytoplasmic Ca²⁺ concentration. During the cardiac cycle, cardiomyocyte contraction and calcium homeostasis are regulated by Ca²⁺ regulatory proteins such as SERCA2 and its regulator PLB^[49]. SERCA2 transports 70% of cytoplasmic Ca²⁺ back to the SR during diastole, which is the main mechanism of Ca²⁺ recycling. SERCA2 activity is positively correlated with cardiac function and negatively correlated with the degree of CaMKII activation^[49,50]. Under normal physiological conditions, SERCA2 activity is inhibited by its binding to PLB. Moreover, the extent of PLB phosphorylation at Thr17 reflects CaMKII activity^[22,51]. After phosphorylation, P-PLB dissociates from SERCA2, thus removing its inhibitory effect on SERCA2^[51]. Numerous studies have shown that ISO can significantly reduce SERCA2 expression and increase PLB phosphorylation in rat myocardial tissue^[52]. Although PLB phosphorylation can increase SERCA2 activity, this effect may be weaker than those of CaMKII and oxidative stress on SERCA2 protein expression, which results in an increase in the Ca²⁺ load in myocardial tissue; this conclusion is consistent with those of Zhebo Liu et al.^[50]. The results of this study confirmed that YXDJ antagonizes VA by decreasing the expression and activity of CaMKII, increasing SERCA2 protein expression, reducing the degree of PLB phosphorylation, and thereby reducing the cytoplasmic Ca²⁺ load.

5. Conclusion

In conclusion, CaMKII was upregulated and SERCA2 was downregulated in the myocardia of rats with ISO-induced VA. YXDJ may reduce the expression of CaMKII, activate SERCA2, and reduce the Ca²⁺ load in myocardial tissue to antagonize VA. The occurrence and extent of YXDJ VA antagonism may be related to the decrease in CaMKII expression, activation of SERCA2, and decrease in the Ca²⁺ load in myocardial tissue. However, how oxidative stress leads to the downregulation of SERCA2 and whether CaMKII directly inhibits SERCA2 expression still need further study.

Acknowledgments

Funding Statement

This work was supported by Key R&D Program of Hebei Province [No.213777550].

References

- [1] Haqqani H M, Chan K H, Kumar S, et al. *The Contemporary Era of Sudden Cardiac Death and Ventricular Arrhythmias: Basic Concepts, Recent Developments and Future Directions*[J]. *Heart Lung Circ*, 2019, 28(1): 1-5.
- [2] Sattler S M, Skibsbbye L, Linz D, et al. *Ventricular Arrhythmias in First Acute Myocardial Infarction: Epidemiology, Mechanisms, and Interventions in Large Animal Models*[J]. *Front Cardiovasc Med*, 2019, 6: 158.
- [3] Hu Z, Wang M, Zheng S, et al. *Clinical Decision Support Requirements for Ventricular Tachycardia Diagnosis Within the Frameworks of Knowledge and Practice: Survey Study*[J]. *JMIR Hum Factors*, 2024, 11: e55802.
- [4] Hayashi T, Tiwary S K, Lavine K J, et al. *The Programmed Death-1 Signaling Axis Modulates Inflammation and LV Structure/Function in a Stress-Induced Cardiomyopathy Model*[J]. *JACC Basic Transl Sci*, 2022, 7(11): 1120-1139.
- [5] Wood B M, Simon M, Galice S, et al. *Cardiac CaMKII activation promotes rapid translocation to its extra-dyadic targets*[J]. *J Mol Cell Cardiol*, 2018, 125: 18-28.
- [6] Ma K, Ma G, Guo Z, et al. *Regulatory mechanism of calcium/calmodulin-dependent protein kinase II in the occurrence and development of ventricular arrhythmia (Review)*[J]. *Exp Ther Med*, 2021, 21(6): 656.
- [7] Huang X, Wang Y, Wang Y, et al. *Ophiopogonin D Reduces Myocardial Ischemia-Reperfusion Injury via Upregulating CYP2J3/EETs in Rats*[J]. *Cell Physiol Biochem*, 2018, 49(4): 1646-1658.
- [8] Zhao Z, Liu M, Zhang Y, et al. *Cardioprotective Effect of Monoammonium Glycyrrhizinate Injection Against Myocardial Ischemic Injury in vivo and in vitro: Involvement of Inhibiting Oxidative Stress and Regulating Ca(2+) Homeostasis by L-Type Calcium Channels*[J]. *Drug Des Devel Ther*, 2020, 14: 331-346.
- [9] Guo Z, Liu G, Ma K, et al. *Antagonistic effect and mechanism of Yangxin Dingji capsule on isoproterenol-induced ischemic arrhythmia in SD rats* [J]. *Traditional Chinese Medicine* Jan 40: 97-269, 2021.
- [10] Zhong Y, Liu G, Ma G, et al. *Myocardial Protective effect of Yangxin Dingpalpitum capsule on golden hamster model of diabetic cardiomyopathy* [J]. *Chinese Pharmacy* 33:1573-1580, 2022.
- [11] Nassal D, Gratz D, Hund T J. *Challenges and Opportunities for Therapeutic Targeting of Calmodulin Kinase II in Heart*[J]. *Frontiers in Pharmacology*, 2020, 11.
- [12] Yang M, Zhang S, Ren S, et al. *Effect of aqueous extract of sanweitanxiang Powder on calcium homeostasis Protein expression in ischemic-reperfusion injury rat heart*[J]. *J Tradit Chin Med*, 2013,33: 355-60, .
- [13] Macala K, Tabrizchi R. *The effect of fat emulsion on hemodynamics following treatment with propranolol and clonidine in anesthetized rats*[J]. *Acad Emerg Med*, 2014, 21(11): 1220-5.
- [14] Guo Z, Zhang N, Ma K, et al. *Establishment of a new arrhythmia model in SD rats induced by isoproterenol*[J]. *Acta Cardiol*, 2023, 78(6): 703-712.
- [15] Feng Y, Cheng J, Wei B, et al. *CaMKII inhibition reduces isoproterenol-induced ischemia and arrhythmias in hypertrophic mice*[J]. *Oncotarget Mar*, 2017,8: 17504-17509 .
- [16] Wang Q W, Yu X F, Xu H L, et al. *Ginsenoside Re Attenuates Isoproterenol-Induced Myocardial Injury in Rats*[J]. *Evid Based Complement Alternat Med*, 2018, 2018: 8637134.
- [17] Almahameed S T, Ziv O. *Ventricular Arrhythmias*[J]. *Med Clin North Am*, 2019, 103(5): 881-895.
- [18] Curtis M J, Hancox J C, Farkas A, et al. *The Lambeth Conventions (II): guidelines for the study of animal and human ventricular and supraventricular arrhythmias*[J]. *Pharmacol Ther*, 2013, 139(2): 213-48.
- [19] Ullah A, Hoang-Trong M T, Lederer W J, et al. *Critical Requirements for the Initiation of a Cardiac Arrhythmia in Rat Ventricle: How Many Myocytes?*[J]. *Cells*, 2022, 11(12).
- [20] Koyani C N, Scheruebel S, Jin G, et al. *Hypochlorite-Modified LDL Induces Arrhythmia and Contractile Dysfunction in Cardiomyocytes*[J]. *Antioxidants (Basel)*, 2021, 11(1).
- [21] Ahmed L A, Hassan O F, Galal O, et al. *Beneficial effects of benfotiamine, a NADPH oxidase inhibitor, in isoproterenol-induced myocardial infarction in rats*[J]. *PLoS One*, 2020, 15(5): e0232413.
- [22] Sun L, Chen Y, Luo H, et al. *Ca(2+)/calmodulin-dependent protein kinase II regulation by*

inhibitor 1 of protein phosphatase 1 alleviates necroptosis in high glucose-induced cardiomyocytes injury[J]. *Biochem Pharmacol*, 2019, 163: 194-205.

[23] Matzer I, Voglhuber J, Kiessling M, et al. *beta-Adrenergic Receptor Stimulation Maintains NCX-CaMKII Axis and Prevents Overactivation of IL6R-Signaling in Cardiomyocytes upon Increased Workload*[J]. *Biomedicines*, 2022, 10(7).

[24] Power A S, Asamudo E U, Worthington L P I, et al. *Nitric Oxide Modulates Ca²⁺ Leak and Arrhythmias via S-Nitrosylation of CaMKII*[J]. *Circulation Research*, 2023, 133(12): 1040-1055.

[25] Wang Y, Huang X, Ma Z, et al. *Ophiopogonin D alleviates cardiac hypertrophy in rat by upregulating CYP2J3 in vitro and suppressing inflammation in vivo*[J]. *Biochem Biophys Res Commun*, 2018, 503(2): 1011-1019.

[26] Yang X, Xiong X, Wang H, et al. *Protective effects of Panax notoginseng saponins on cardiovascular diseases: a comprehensive overview of experimental studies*[J]. *Evid Based Complement Alternat Med* 2014: 204840, 2014.

[27] Gou D, Pei X, Wang J, et al. *Antiarrhythmic effects of ginsenoside Rg2 on calcium chloride-induced arrhythmias without oral toxicity*[J]. *J Ginseng Res*, 2020, 44(5): 717-724.

[28] Guevorkian A G. *The effect of hypothalamic peptides, neurohormone C and proline-rich peptide-Ion the Ca(2+)-handling system in heartin pathophysiological conditions*[J]. *Heliyon*, 2020, 6(6): e04360.

[29] Wang S, Wang X, Ling L, et al. *RICH1 is a novel key suppressor of isoproterenol- or angiotensin II-induced cardiomyocyte hypertrophy*[J]. *Mol Med Rep*, 2024, 29(5).

[30] Chu J, Zhou X, Peng M, et al. *Huoxin Pill Attenuates Cardiac Inflammation by Suppression of TLR4/NF-kappaB in Acute Myocardial Ischemia Injury Rats*[J]. *Evid Based Complement Alternat Med*, 2020, 2020: 7905902.

[31] Song L, Srilakshmi M, Wu Y, et al. *Sulforaphane Attenuates Isoproterenol-Induced Myocardial Injury in Mice*[J]. *Biomed Res Int*, 2020, 2020: 3610285.

[32] Adameova A, Shah A K, Dhalla N S. *Role of Oxidative Stress in the Genesis of Ventricular Arrhythmias*[J]. *Int J Mol Sci*, 2020, 21(12).

[33] Afzal M R, Savona S, Mohamed O, et al. *Hypertension and Arrhythmias*[J]. *Heart Failure Clinics*, 2019, 15(4): 543-550.

[34] Kura B, Szeiffova Bacova B, Kalocayova B, et al. *Oxidative Stress-Responsive MicroRNAs in Heart Injury*[J]. *Int J Mol Sci*, 2020, 21(1).

[35] Bostan M M, Stasescu C, Anghel L, et al. *Post-Myocardial Infarction Ventricular Remodeling Biomarkers-The Key Link between Pathophysiology and Clinic*[J]. *Biomolecules*, 2020, 10(11).

[36] Thangaiyan R, Arjunan S, Govindasamy K, et al. *Galangin Attenuates Isoproterenol-Induced Inflammation and Fibrosis in the Cardiac Tissue of Albino Wistar Rats*[J]. *Front Pharmacol*, 2020, 11: 585163.

[37] Ping P, Yang T, Ning C, et al. *Chlorogenic acid attenuates cardiac hypertrophy via up-regulating Sphingosine-1-phosphate receptor1 to inhibit endoplasmic reticulum stress*[J]. *ESC Heart Fail*, 2024.

[38] Eltobshy S a G, Hussein A M, Elmileegy A A, et al. *Effects of heme oxygenase-1 upregulation on isoproterenol-induced myocardial infarction*[J]. *Korean J Physiol Pharmacol*, 2019, 23(3): 203-217.

[39] Habte-Tsion H M, Kolimadu G D, Rossi W, Jr., et al. *Effects of Schizochytrium and micro-minerals on immune, antioxidant, inflammatory and lipid-metabolism status of Micropterus salmoides fed high- and low-fishmeal diets*[J]. *Sci Rep*, 2020, 10(1): 7457.

[40] Othman A I, Elkomy M M, El-Missiry M A, et al. *Epigallocatechin-3-gallate prevents cardiac apoptosis by modulating the intrinsic apoptotic pathway in isoproterenol-induced myocardial infarction*[J]. *Eur J Pharmacol*, 2017, 794: 27-36.

[41] Zhou Y, Liu L, Gao C, et al. *Puerarin pre-conditioning on the expression levels of CK-MB, cTnI and inflammatory factors in patients undergoing cardiac valve replacement*[J]. *Exp Ther Med*, 2019, 17(4): 2598-2602.

[42] Cabral P D, Silva G B, Baigorria S T, et al. *Nitric oxide-inhibited chloride transport in cortical thick ascending limbs is reversed by 8-iso-prostaglandin-F2alpha*[J]. *Kidney Res Clin Pract*, 2022, 41(6): 699-706.

[43] Pu Y, Wu D, Lu X, et al. *Effects of GCN2/eIF2alpha on myocardial ischemia/hypoxia reperfusion and myocardial cells injury*[J]. *Am J Transl Res*, 2019, 11(9): 5586-5598.

[44] Xie W, Hou G, Wang L, et al. *Astaxanthin suppresses lipopolysaccharide-induced myocardial injury by regulating MAPK and PI3K/AKT/mTOR/GSK3β signaling* [J]. *Mol Med Rep* 22:3338-3346, 2020.

[45] Xu M, Li X, Song L. *Baicalin regulates macrophages polarization and alleviates myocardial ischaemia/reperfusion injury via inhibiting JAK/STAT pathway*[J]. *Pharm Biol*, 2020, 58(1): 655-663.

[46] El-Sayed S F, Abdelhamid A M, Zeinelabdeen S G, et al. *Melatonin enhances captopril mediated*

cardioprotective effects and improves mitochondrial dynamics in male Wistar rats with chronic heart failure[J]. *Sci Rep*, 2024, 14(1): 575.

[47] Wang Q, Quick A P, Cao S, et al. Oxidized CaMKII (Ca(2+)/Calmodulin-Dependent Protein Kinase II) Is Essential for Ventricular Arrhythmia in a Mouse Model of Duchenne Muscular Dystrophy[J]. *Circ Arrhythm Electrophysiol*, 2018, 11(4): e005682.

[48] Li J, Wang S, Zhang J, et al. The CaMKII phosphorylation site Thr1604 in the CaV1.2 channel is involved in pathological myocardial hypertrophy in rats[J]. *Channels (Austin)*, 2020, 14(1): 151-162.

[49] Li K, Guo C, Ruan J, et al. Cadmium Disrupted ER Ca(2+) Homeostasis by Inhibiting SERCA2 Expression and Activity to Induce Apoptosis in Renal Proximal Tubular Cells[J]. *Int J Mol Sci*, 2023, 24(6).

[50] Liu Z, Tao B, Fan S, et al. Over-expression of microRNA-145 drives alterations in β -adrenergic signaling and attenuates cardiac remodeling in heart failure Post myocardial infarction [J]. *Aging (Albany NY)* 12: 11603-11622, 2020.

[51] Lee T I, Trang N N, Lee T W, et al. Ketogenic Diet Regulates Cardiac Remodeling and Calcium Homeostasis in Diabetic Rat Cardiomyopathy[J]. *Int J Mol Sci*, 2023, 24(22).

[52] Romero-Garcia T, Landa-Galvan H V, Pavon N, et al. Autonomous activation of CaMKII exacerbates diastolic calcium leak during beta-adrenergic stimulation in cardiomyocytes of metabolic syndrome rats[J]. *Cell Calcium*, 2020, 91: 102267.